EUROPEAN JOURNAL OF PURE AND APPLIED MATHEMATICS
Vol. 17, No. 4, 2024, 3167-3184
ISSN 1307-5543 – ejpam.com
Published by New York Business Global

Designing an Efficient Numerical Method for Solving the Blood Ethanol Concentration System and Ebola Virus Models

Mohamed M. Khader[1,2,*], Mohammed M. Babatin[1]

[1] *Department of Mathematics and Statistics, College of Science, Imam Mohammad Ibn Saud Islamic University (IMSIU), Riyadh, Saudi Arabia*
[2] *Department of Mathematics, Faculty of Science, Benha University, Benha, Egypt*

Abstract. This study aims to provide a numerical simulation of two important models called the Blood Ethanol Concentration (BEC) model and the Ebola Virus model in their fractional form (Caputo-Fabrizio sense (CF)). Here, we used Simpson's 1/3 rule as an efficient numerical scheme for integration to solve the obtained fractional integral equations (FIEs) and reduce it to a collection of algebraic equations. Particular emphasis is placed on elucidating the error analysis of the given scheme. The results acquired by implementing the Runge-Kutta method (RK4M) and others are compared to the achieved results. The results explain that the implemented scheme offers a straightforward and effective tool for simulating solutions of these models. The primary benefit of the implemented method is that it relies on a small number of uncomplicated steps and does not have long-term effects. Finally, numerical simulations support the theoretical conclusions, showing the great agreement between the two.

2020 Mathematics Subject Classifications: 34A12, 41A30, 26C10, 47H10, 65N20

Key Words and Phrases: Blood ethanol concentration system, Ebola virus epidemic model, Caputo-Fabrizio fractional derivative, Numerical integration, RK4M

1. Introduction

Given the importance of modeling and analyzing many problems in the mathematical life sciences, which in turn provide many different data concerning biological phenomena such as the bacterial cell and its allocation, the nervous system, viruses (such as the Ebola virus), etc. ([4], [22]), we found that many researchers have recently focused on this branch of science. These mathematical models of numerous real-world issues are derived and formulated depending on the results of many biological experiments or statistical analyzes. These mathematical models enable scientists to study and simulate the behavior of these

*Corresponding author.
DOI: https://doi.org/10.29020/nybg.ejpam.v17i4.5447

Email addresses: mmkhader@imamu.edu.sa (M. M. Khader), mmbabatin@imamu.edu.sa (M. M. Babatin)

realistic models, separate from modern biological experiments conducted in laboratories, which may pose risks or be very costly ([5], [23]).

Ebola virus disease (EVD) was first revealed in 1976 in the Congo near the Ebola River. Although this disease is rare, it often causes death [22]. The EVD infects monkeys and humans on and off, and it also leads to outbreaks in some other African countries. However for some time, it has been complicated for numerous biologists to locate the original origin of the virus; but, through recent studies and experiments, it has been set up that it is foremost transmitted from animals such as bats meaning that they are the origin of the EVD [16]. In general, this virus can infect humans during immediate connection with humans, the blood or body fluids of a sick or deceased person, or animal tissues [18]. Recent studies have confirmed that EVD can pass during broken skin or mucous membranes in the eyes, nose, and mouth when a person comes into connect with the body fluids of an infected person. It can also be moved during sexual contact with a person infected with the virus or who has recovered from it [7].

Scientists are currently studying more effective fractional operators. In order to address the issue of singularity and achieve accurate and reliable modeling outcomes, a more effective CF fractional derivative has been developed. This derivative incorporates a non-singular kernel, as proposed by Caputo and Fabrizio, leading to improved efficiency and robustness in recent years. The use of Laplace transformation to convert it to integer power is regarded as a constructive method. Time-fractional Caputo-Fabrizio fractal fractional derivatives (with an exponential decay kernel) are applied to the Burke-Shaw-type nonlinear chaotic systems. Based on fixed point theory, it has been demonstrated that such an operator exists and is unique [24]. The author solved this model by using a numerical power series method with Newton's interpolation polynomials. In the paper [3], the authors proposed some updated and improved numerical schemes based on Newton's interpolation polynomial to solve numerically the Burke-Shaw system of Caputo's time-fractal fractional derivative with a power-law kernel with variable order. Additionally, they calculated the Lyapunov exponent of the proposed system. Furthermore, the Atangana-Seda numerical scheme, based on Newton polynomials, has been used to solve this problem. The authors proposed a generalized numerical scheme by using the Lagrange polynomial interpolation to simulate variable-order fractional differential operators. Two methods, Atangana-Baleanu-Caputo and Atangana-Seda derivatives, were used to solve a chaotic Newton-Leipnik system problem. The fractional-order epidemic model of the hepatitis C virus (HCV) involving partial immunity under the influence of memory effect to know the transmission patterns and prevalence of HCV infection is studied in [17]. The authors calculated the basic reproduction number for the HCV model using the next-generation matrix technique to determine the model's global dynamics. The model's reproduction number shows how the disease progresses. The model's numerical solutions are obtained using the fractional Adams method. The study in [20] introduced a family of root-solvers for systems of nonlinear equations, leveraging the Daftardar-Gejji and Jafari decomposition technique coupled with the midpoint quadrature rule. Also, they presented a comprehensive analysis of their stability and semi-local convergence with the help of Taylor series expansions and the Banach fixed point theorem. The practical efficacy and applica-

bility of the developed methods are demonstrated through the resolution of five real-world application problems of complex nonlinear systems.

Many mathematicians find it challenging to create numerical and approximate solutions for the FDEs [11]. The Adams-Bashforth method, incorporating the CF operator, is formulated in [19]. This method involves three steps and can be used to solve both linear/nonlinear FDEs. Additionally, it possesses diverse uses in resolving chaotic systems with fractional orders. The study [2] introduced a fractional MSD model that incorporates CF-derivatives. The authors [10] have developed a trapezoidal strategy to solve the FDEs efficiently. This scheme utilizes the CF operator and achieves a convergence order of two. Additionally, the convergence and stability of this technique have been thoroughly investigated. Inspired by this research, we devised Simpson's 1/3 scheme for solving FDEs. This method achieves a high level of accuracy, with an order of four, as detailed in our work. The proposed fractional Simpson's 1/3 approach offers superior accuracy compared to current methods and is straightforward to implement.

2. Preliminaries

Mathematical models using more accurate fractional derivatives (FD) have been used by taking advantage of a non-singular kernel. This approach enhances the system's ability to accurately represent and capture memory effects. In 2015, Caputo and Fabrizio successfully introduced the CF-fractional derivative by substituting the singular kernel $(t-\tau)^{-\gamma}$ with $e^{\left(\frac{-\gamma(t-\tau)}{1-\gamma}\right)}$ in the Caputo derivative [8]. Here, we will provide a succinct overview of fundamental definitions pertaining to fractional calculus involving a non-singular kernel.

Definition 1.

For $\psi(t) \in \mathbb{H}^1(0,a), 0<\gamma<1$. Then the CF-FD, ${}^{CF}D^{\gamma}\psi(t)$ and CF-fractional integral ${}^{CF}I^{\gamma}\psi(t)$, respectively are defined by:

$$
\begin{aligned}
{}^{CF}D^{\gamma}\psi(t) &:= \frac{1}{1-\gamma}\int_0^t \mathrm{Exp}\Big[-\frac{\gamma}{1-\gamma}(t-\tau)\Big]\dot{\psi}(\tau)d\tau,\\
{}^{CF}I^{\gamma}\psi(t) &:= (1-\gamma)\psi(t)+\gamma\int_0^t \psi(\tau)d\tau. \qquad (1)
\end{aligned}
$$

3. Formulation of the two models

3.1. Description of the blood ethanol concentration model

Here, we will use the experimental study conducted in [15] to deduce the mathematical model that describes the issue under study to locate the concentration of alcohol in the human stomach $\theta_1(t)$ & in his blood $\theta_2(t)$ at any time t (mg/l), as it is the major provenance for obtaining the real data for the present study. The proposed system in its CF-fractional

form is specified by the subsequent equations:

$$\begin{aligned} {}^{CF}D^{\alpha}\theta_1(t) &= -\lambda^{\alpha}\theta_1(t), \\ {}^{CF}D^{\beta}\theta_2(t) &= \lambda^{\beta}\theta_1(t) - \mu^{\beta}\theta_2(t), \end{aligned} \tag{2}$$

$$\theta_1(0) = \theta_1^0, \qquad \theta_2(0) = 0,$$

where λ and μ are the rate law constants 1 and 2, respectively [15].
The true solution of this model is defined by [21]:

$$\begin{aligned} \theta_1(t) &= \theta_1^0\, E_{\alpha}(-\lambda^{\alpha}t^{\alpha}), \\ \theta_2(t) &= \theta_1^0\lambda^{\beta}\sum_{p=0}^{\infty}\sum_{q=0}^{\infty}\frac{(-\lambda^{\alpha})^p(-\mu^{\beta})^q}{\Gamma(p\alpha+q\beta+\beta+1)}t^{p\alpha+q\beta+\beta}. \end{aligned}$$

3.2. Description of the Ebola virus disease model

The fractional epidemiological system (with the total population, N) of the EVD can be described as follows [9]:

$$\begin{aligned} {}^{CF}D^{\nu}\psi_1(t) &= -\alpha\,\psi_1(t)\,\psi_2(t) + \beta\,\psi_3(t) - \gamma\,N, \\ {}^{CF}D^{\nu}\psi_2(t) &= \alpha\,\psi_1(t)\,\psi_2(t) - \epsilon\,\psi_2(t) - \delta\,\psi_2(t), \\ {}^{CF}D^{\nu}\psi_3(t) &= \delta\,\psi_2(t) - \beta\,\psi_3(t), \\ {}^{CF}D^{\nu}\psi_4(t) &= \epsilon\,\psi_2(t) + \gamma\,N, \end{aligned} \tag{3}$$

with the I.Cs $\psi_i(0) = \hat{\psi}_i^0$, $i = 1, 2, 3, 4$ where $\nu \in (0, 1]$. All variables & constants contained in the previous model can be described & defined as in the following table:

Symbol	Description
$\psi_1(t)$, $\psi_2(t)$ and $\psi_3(t)$	The susceptible, infected, and recovery population, respectively
$\psi_4(t)$	The population died
α	The rate of infection with the disease
β and γ	The rate of susceptibility, and natural death respectively
ϵ and δ	The rate of death, and recovery from the disease, respectively

Throughout the examination of the models presented in (2) and (3), the subsequent approaches will be employed. We will provide the necessary definitions in the following sections. The advanced portions will then contain numerical results, simulations, and conclusions. The study's primary goal is to examine the models under the CF-fractional derivative.

4. Derivation Simpson's-1/3 rule for CF-fractional integral

This section presents the formulation of the fractional Simpson's-1/3 rule (FSR) for solving CF-FDEs [6]. This aim will be achieved through the following steps:

(i) Considering the subsequent γ-order IVP:

$$^{CF}D^{\gamma}u(t) = f(u(t)), \qquad u(0) = u_0. \tag{4}$$

(ii) Applying the CF-fractional integral operator on the IVP (4) and applying Proposition 3 in [1] and formula (1), we get:

$$u(t) = u_0 + {}^{CF}I^{\gamma} f\left(u(t)\right) = u_0 + (1-\gamma)f(u(t)) + \gamma \int_0^t f(u(s))ds. \tag{5}$$

(iii) Initially, we will employ a quadratic polynomial P_2 to estimate the integral function f in Equation (5). The function will be assessed at t_0, t_1, and t_2, where t_0 is less than t_1 and t_1 is less than t_2. The interval is partitioned into two subintervals, denoted as $t_1 - t_0 = t_2 - t_1 = h$, resulting in a combined width of $2h$. The integration of the quadratic polynomial P_2 can be computed as follows:

$$I_2 f(u(t)) = \int_a^b f(u(t))dt \approx \int_{t_0}^{t_2} P_2(u(t))dt = \int_{t_0}^{t_2} \left[\sum_{j=0}^{2} L_j(t)\, f\left(u\left(t_j\right)\right)\right] dt,$$

where the second-order Lagrange polynomials $L_0(t)$, $L_1(t)$, and $L_2(t)$ are defined as follows:

$$L_j(t) = \prod_{i=0,\, i\neq j}^{2} \frac{(t-t_i)}{(t_j - t_i)}.$$

(iv) Integrating the first interpolant function $L_0(t)$, by taking $h = \frac{t_2 - t_0}{2}$ and substituting "$t = s + t_0$", gives us:

$$\begin{aligned}\int_{t_0}^{t_2} L_0(t)dt &= \frac{1}{2h^2}\int_{t_0}^{t_0+2h} (t-t_1)\,(t-t_2)\,dt = \frac{1}{2h^2}\int_0^{2h} (s+t_0-t_2)\,(s+t_0-t_1)\,ds \\ &= \frac{1}{2h^2}\int_0^{2h} (s-2h)(s-h)ds = \frac{h}{3}.\end{aligned}$$

After making some simplifications to the rest of the terms, we have the following:

$$I_2(f) = \frac{h}{3}\left[f\left(u\left(t_0\right)\right) + 4f\left(u\left(t_1\right)\right) + f\left(u\left(t_2\right)\right)\right].$$

(v) By substituting in the equation (5), we get:

$$u\left(t_n\right) = u_0 + (1-\gamma)f\left(u\left(t_n\right)\right) + \frac{h}{3}\left[f\left(u\left(t_0\right)\right) + 4f\left(u\left(t_1\right)\right) + f\left(u\left(t_2\right)\right)\right], \quad n = 0, 1, 2.$$

(vi) To improve the accuracy of numerical integration, we partition $[a,b]$ to n subintervals as follows:
For any even number $n \geq 2$, we establish the following definitions:

$$h = \frac{b-a}{n} = t_{k+1} - t_k, \quad k = 0, 1, 2, \ldots, n.$$

Now, by using the quadrature rule for each pair of subintervals and implementing the Simpson's-1/3 rule to each of $\left[t_{2k}, t_{2(k+1)}\right], \quad k = 0, 1, 2, \ldots, \frac{n-2}{2}$, we can appoint the following formula:

$$I_n(f) = \sum_{k=0}^{\frac{n-2}{2}} \int_{t_{2k}}^{t_{2k+2}} f(u(t))dt = \sum_{k=0}^{\frac{n-2}{2}} \left(\frac{h}{3} \left[f\left(u\left(t_{2k}\right)\right) + 4f\left(u\left(t_{2k+1}\right)\right) + f\left(u\left(t_{2k+2}\right)\right) \right] \right).$$

(vii) By referring u_j as the approximate solution of $u\left(t_j\right)$ and using Eq.(5), we can write the FSR for the CF-FDE (4), for $j = 0[1](n-1)$:

$$u_{j+1} = u_0 + (1-\gamma) f\left(u_{j+1}\right) + \gamma \frac{h}{3} \left[f\left(u\left(t_0\right)\right) + 4 \sum_{i=2,4,6}^{j} f\left(u\left(t_i\right)\right) + 2 \sum_{j=1,3,5}^{j-1} f\left(u\left(t_j\right)\right) + f\left(u\left(t_{j+1}\right)\right) \right].$$

This formula can be rewritten in a compact form as follows:

$$u_{j+1} = u_0 + (1-\gamma) f\left(u_{j+1}\right) + \gamma\, h \sum_{r=0}^{j+1} \xi_r\, f\left(u_r\right), \qquad j = 0, 1, 2, \ldots, n-1, \tag{6}$$

where ξ_r are the weights of the FSR and are defined as:

$$\xi_r = \begin{cases} 1/3, & r = 0,\ n+1, \\ 2/3, & r = 1, 3, 5, \ldots, \\ 4/3, & r = 2, 4, 6, \ldots. \end{cases}$$

5. Convergence analysis

In this section, we are going to collect some theorems concerning the stability and error analysis of the given IVP (4), and the regulated numerical scheme which investigated and proved in ([6], [14]).

Theorem 1. *[14]*

Let us assume a continuous function f: $[0,T] \times \mathbb{R} \to \mathbb{R}$ with $\gamma \in (0,1)$ that satisfies the Lipschitz condition:

$$|f\left(u(t_1)\right) - f\left(u(t_2)\right)| \leq \epsilon\, |u(t_1) - u(t_2)|, \qquad \epsilon > 0. \tag{7}$$

Then the IVP (4) has a unique solution on $C[0,T]$ under the condition:

$$\frac{(2(1-\gamma) + 2\gamma T)\epsilon}{(2-\gamma)} < 1.$$

Lemma 1.

Suppose that $f(u(t)) \in C^4([a,b])$, then the error of numerical scheme (6) is estimated by:

$$\left| \int_{t_0}^{t_{n+1}} f(u(s))ds - \gamma h \sum_{i=0}^{n+1} \xi_i f\left(u(t_i)\right) \right| \leq h^4,$$

where $\hat{c} = \frac{(b-a)f^{(4)}(\zeta)}{180}$, for some constant $a < \zeta < b$, $h = \frac{b-a}{n}$, and $t_k = a + hk$, $k = 0, 1, \ldots, n+1$.
The stability and error analysis of the regulated numerical scheme are investigated and proved meanwhile the following theorems [6].

Theorem 2.

The newly designed fractional numerical technique (6) exhibits conditional stability.

Theorem 3.

The recently developed fractional numerical method exhibits conditional convergence of order four, as stated in the equation (6):

$$\|u\left(t_{n+1}\right) - u_{n+1}\| \leq \mathfrak{C} h^4,$$

where $\mathfrak{C} = \gamma \hat{c}\, c_h$.

6. Numerical implementation

Here in this section, we will try to treat the shortcomings of the existing numerical methods, which are represented by the slow convergence of most of them when solving this type of problem, which in turn leads to inaccurate approximations [13]. To address this, we use the FSR for numerical integration to calculate the resulting integral in the system of FIEs obtained from the same models of FDEs under study.

6.1. Solving fractional blood ethanol concentration model

Now, we will numerically treat the BEC system in its fractional form by creating a numerical scheme for it. For this purpose, let us reformulate the system (2) in an operator form as follows:

$$^{CF}D^{\nu}\,\bar{\Theta}(t) = \mathbb{F}(\bar{\Theta}(t), t), \tag{8}$$

where

$$\bar{\Theta}(t) = [\theta_1(t), \theta_2(t)]^T, \qquad \mathbb{F}(\bar{\Theta}(t), t) = [\mathbf{f}_1, \mathbf{f}_2]^T, \qquad \bar{\Theta}(0) = [\theta_1^0, 0]^T, \tag{9}$$

where each one of the functions $\mathbf{f}_i(\theta_1, \theta_2)$, $i = 1, 2$ are defined in the RHS of the two equations in (2), respectively.

Applying the CF-fractional integral operator on the model (8) and implementing Proposition 3 in [1] and formula (1), we get:

$$\bar{\Theta}(t) = \bar{\Theta}(0) + {}^{CF}I^{\nu}\,\mathbb{F}(\bar{\Theta}(t), t) = \bar{\Theta}(0) + (1-\nu)\mathbb{F}(\bar{\Theta}(t), t) + \nu \int_0^t \mathbb{F}(\bar{\Theta}(s), s)ds. \quad (10)$$

Applying the derived FSR for the integration on the RHS of (10), to get the following numerical scheme as constructed in the formula (6):

$$\bar{\Theta}_{j+1} = \bar{\Theta}(0) + (1-\nu)\mathbb{F}(\bar{\Theta}_{j+1}, t_{j+1}) + \nu\, h \sum_{r=0}^{j+1} \xi_r\, \mathbb{F}(\bar{\Theta}_r, t_r), \quad j = 0, 1, 2, \ldots, n-1, \quad (11)$$

where the weights ξ_r, $r = 0, 1, ..., n+1$ of the FSR are defined in (6).

So, the system given in (2) transforms into an algebraic equations system as follows:

$$\theta_{k,j+1} = \theta_{k,0} + (1-\nu)\mathbf{f}_k(\theta_{1,j+1}, \theta_{2,j+1}, t_{j+1}) + \nu\, h \sum_{r=0}^{j+1} \xi_r\, \mathbf{f}_k(\theta_{1,r}, \theta_{2,r}, t_r), \quad k = 1, 2, \quad (12)$$

where the functions $\mathbf{f}_k$ are defined in (9).

6.2. Solving fractional Ebola virus disease model

Now, we will numerically treat the Ebola Virus system in its fractional form by creating a numerical scheme of it. For this purpose, let us reformulate the system (3) in an operator form as follows:

$$^{CF}D^{\nu}\,\bar{\Psi}(t) = \mathbb{F}(\bar{\Psi}(t), t), \quad (13)$$

$$\bar{\Psi}(t) = [\psi_1(t), \psi_2(t), \psi_3(t), \psi_4(t)]^T, \quad \mathbb{F}(\bar{\Psi}(t), t) = [\mathbf{f}_1, \mathbf{f}_2, \mathbf{f}_3, \mathbf{f}_4]^T, \quad \bar{\Psi}(0) = [\hat{\psi}_1^0, \hat{\psi}_2^0, \hat{\psi}_3^0, \hat{\psi}_4^0]^T, \quad (14)$$

where each one of the functions $\mathbf{f}_i(\psi_1, \psi_2, \psi_3, \psi_4)$, $i = 1(1)4$ are defined in the RHS of the four equations in (3), respectively.

Applying the CF-fractional integral operator on the model (13) and implementing Proposition 3 in [1] and formula (1), we get:

$$\bar{\Psi}(t) = \bar{\Psi}(0) + {}^{CF}I^{\nu}\,\mathbb{F}(\bar{\Psi}(t), t) = \bar{\Psi}(0) + (1-\nu)\mathbb{F}(\bar{\Psi}(t), t) + \nu \int_0^t \mathbb{F}(\bar{\Psi}(s), s)ds. \quad (15)$$

Applying the derived FSR for the integration on the RHS of (15), to get the following numerical scheme as constructed in the formula (6):

$$\bar{\Psi}_{j+1} = \bar{\Psi}(0) + (1-\nu)\mathbb{F}(\bar{\Psi}_{j+1}, t_{j+1}) + \nu\, h \sum_{r=0}^{j+1} \xi_r\, \mathbb{F}(\bar{\Psi}_r, t_r), \quad j = 0, 1, 2, \ldots, n-1, \quad (16)$$

where the weights ξ_r, $r = 0, 1, ..., n+1$ of the FSR are defined in (6).
So, the system given in (3) transforms into an algebraic equations system as follows:

$$\begin{aligned}\psi_{k,j+1} = \psi_{k,0} &+ (1-\nu)\mathbf{f}_k(\psi_{1,j+1}, \psi_{2,j+1}, \psi_{3,j+1}, \psi_{4,j+1}, t_{j+1}) \\ &+ \nu\, h \sum_{r=0}^{j+1} \xi_r\, \mathbf{f}_k(\psi_{1,r}, \psi_{2,r}, \psi_{3,r}, \psi_{4,r}, t_r), \qquad k = 1(1)4,\end{aligned} \tag{17}$$

where the functions $\mathbf{f}_k$ are defined in (14).

7. Numerical simulation

7.1. For the blood ethanol concentration model

Here, we behold the model (2) with different values of α, β, n at $\lambda = 0.018713$ and $\mu = 0.084457$ and initial conditions $\theta_1^0 = 500$, $\theta_2^0 = 0$ in [0,100]. We give a numerical simulation for the BEC system by implementing the indicated scheme during in Figures 1-4 [12].

(i) Figure 1 recognizes a comparison between the numerical and true solutions with $\alpha = 0.95$, $\beta = 0.95$, & $n = 200$.

(ii) Figure 2 gives the absolute true error (ATE) with $\alpha = 0.9$, $\beta = 0.9$, & $n = 250$.

(iii) Figure 3 shows the influence of the fractional order on the numerical solution with various values of $\alpha = \beta = 1$, 0.85, 0.75, 0.65 with $n = 200$.

(iv) Figure 4 shows the influence of the fractional order on the numerical solution with various values of $\alpha = \beta = 0.55$, 0.45, 0.35, 0.25 with $n = 200$.

By looking closely at these four figures, we can assert and confirm that the numerical solution is based on the different values of α and β; it is a clear indication that the presented numerical scheme has been well implement for solving the suggested system in its fractional form and with this type of derivatives with small and large values of the fractional order.

In addition, to verify the numerical convergence of the solutions in the interval $[0, 100]$, the fractional trapezoidal rule (FTR) for the numerical integration which achieves a convergence order of two is applied to solve the given problem as the benchmarking to the proposed FSR in terms of efficiency and accuracy [10]. In Table 1, we computed the maximum absolute approximate errors (AAE) to show the performance of the FSR method against the benchmark method in solving the BEC model at various values of the fractional order α, β and the step size h. Table 1 shows that the maximum AAE decreases when the step-size used in the computation decreases. Therefore, the errors illustrated sufficient proof of numerical convergence of the proposed numerical scheme. This comparison confirms the thoroughness of the proposed method in this article.

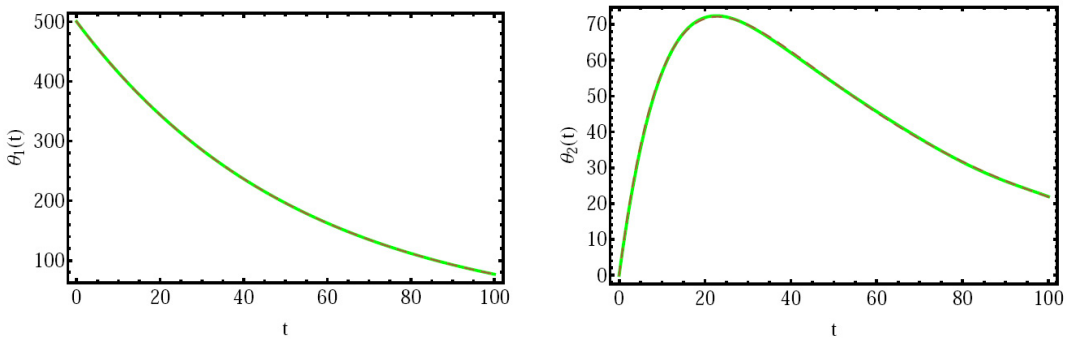

Figure 1. The numerical and true solutions with $\alpha = 0.95$, $\beta = 0.95$, & $n = 200$.

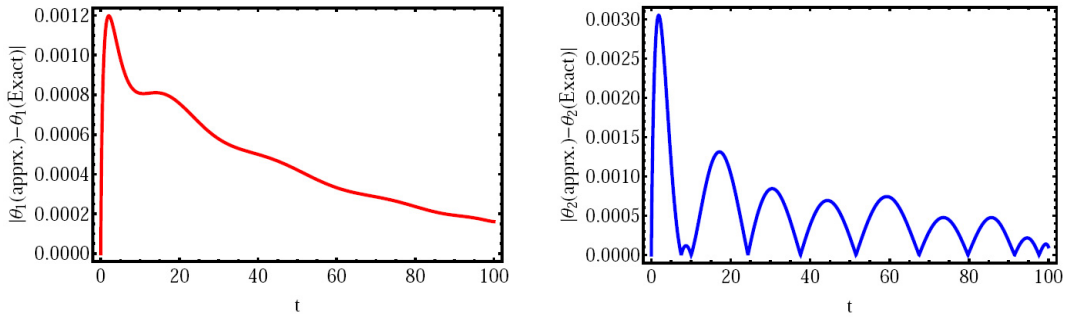

Figure 2: The ATE with $\alpha = 0.9$, $\beta = 0.9$, and $n = 250$.

Table 1. A comparison of the maximum absolute approximate errors from solving the BEC model at different values of α, β, and h.

Method	α/h	$\frac{1}{2}$	$\frac{1}{3}$	$\frac{1}{4}$	$\frac{1}{5}$	$\frac{1}{6}$
FSR	0.75	0.1345E-2	5.9510E-2	8.2140E-3	5.6064E-3	3.5641E-4
FTR		2.0134E-1	6.2581E-1	9.3628E-2	5.9012E-2	3.9752E-2
FSR	0.85	3.2590E-2	9.0560E-2	6.2540E-3	1.5348E-3	1.0654E-4
FTR		3.9521E-1	9.9854E-1	6.9510E-2	1.6542E-2	1.9875E-3
FSR	0.95	7.9325E-2	6.0259E-2	7.0254E-3	3.2541E-3	0.0254E-4
FTR		8.0265E-1	5.2361E-1	8.0124E-2	3.9651E-2	0.9687E-3

7.2. For the Ebola virus disease model

Here, we behold the model (3) with various quantities of ν, n, α, β, γ, δ, ϵ, N in $[0, 5]$. We take two cases of the I.Cs ψ_i^0, $i = 1, 2, 3, 4$ as follows [25]:

(i) **Case 1:** $\psi_1^0 = 100, \quad \psi_2^0 = 10, \quad \psi_3^0 = 0, \quad \psi_4^0 = 0;$

(ii) **Case 2:** $\psi_1^0 = 70, \quad \psi_2^0 = 2, \quad \psi_3^0 = 0, \quad \psi_4^0 = 0.$

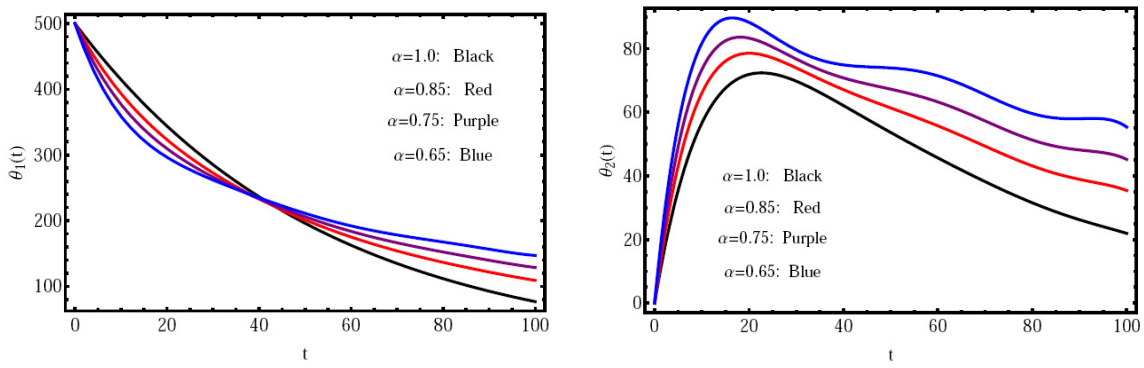

Figure 3: The numerical solution with various values of $\alpha > 0.55$ & $\beta > 0.55$ with $n = 200$.

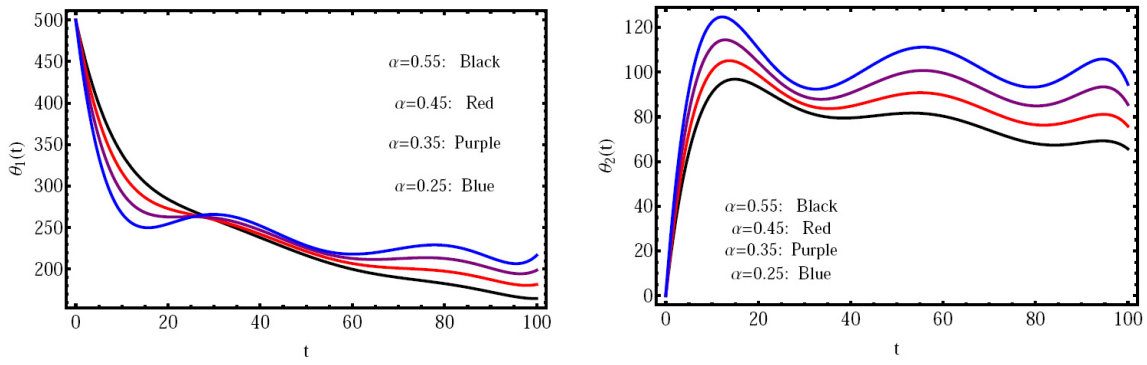

Figure 4: The numerical solution with various values of $\alpha \leq 0.55$ & $\beta \leq 0.55$ with $n = 200$.

We give a numerical simulation for the EVD system by implementing the indicated scheme during in Figures 5-9.

(i) Figure 5 recognizes a comparison between the numerical solution by the proposed scheme & the solution by RK4M (at $\nu = 1$) with $\alpha = 0.001$, $\gamma = 0.01$, $\beta = 0.002$, $\epsilon = 0.006$, $\delta = 0.004$, & $n = 40$, the I.Cs are given by Case 2.

(ii) Figure 6 gives a comparison between the numerical solutions by the introduced scheme and the approximate solution by applying the scheme in [25] at $\nu = 0.9$ with the I.Cs given by Case 1, and the values of β, α, γ, δ, ϵ, n are the same in Figure 5.

(iii) Figure 7 gives the relative approximate error (RAE) with $\nu = 0.95$ for the values $n = 40$, $\alpha = 0.01$, $\beta = 0.02$, $\gamma = 0.01$, $\epsilon = 0.6$, $\delta = 0$,, with I.Cs given by Case 1.

(iv) Figure 8 shows the impact of the fractional order ν on the numerical solution with various quantities of $\nu = 1, 0.9, 0.8, 0.7$, with I.Cs given by Case 2, and the values of β, α, γ, δ, ϵ, n are the same in Figure 5.

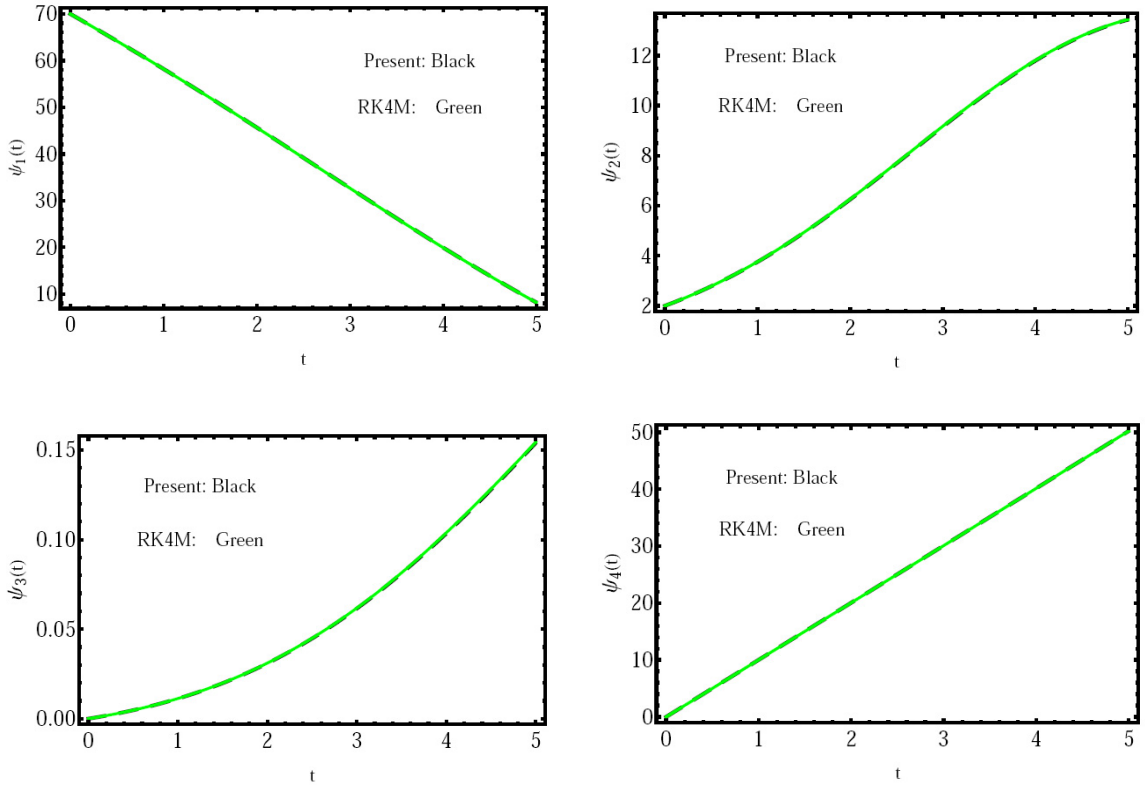

Figure 5. Comparison between the obtained numerical solutions & the RK4M with the I.Cs given by Case 2.

(v) Figure 9 shows the impact of the fractional order ν on the numerical solution with various quantities of $\nu = 0.5, 0.4, 0.3, 0.2$, with I.Cs given by Case 2, and the values of β, α, γ, δ, ϵ, n are the same in Figure 5.

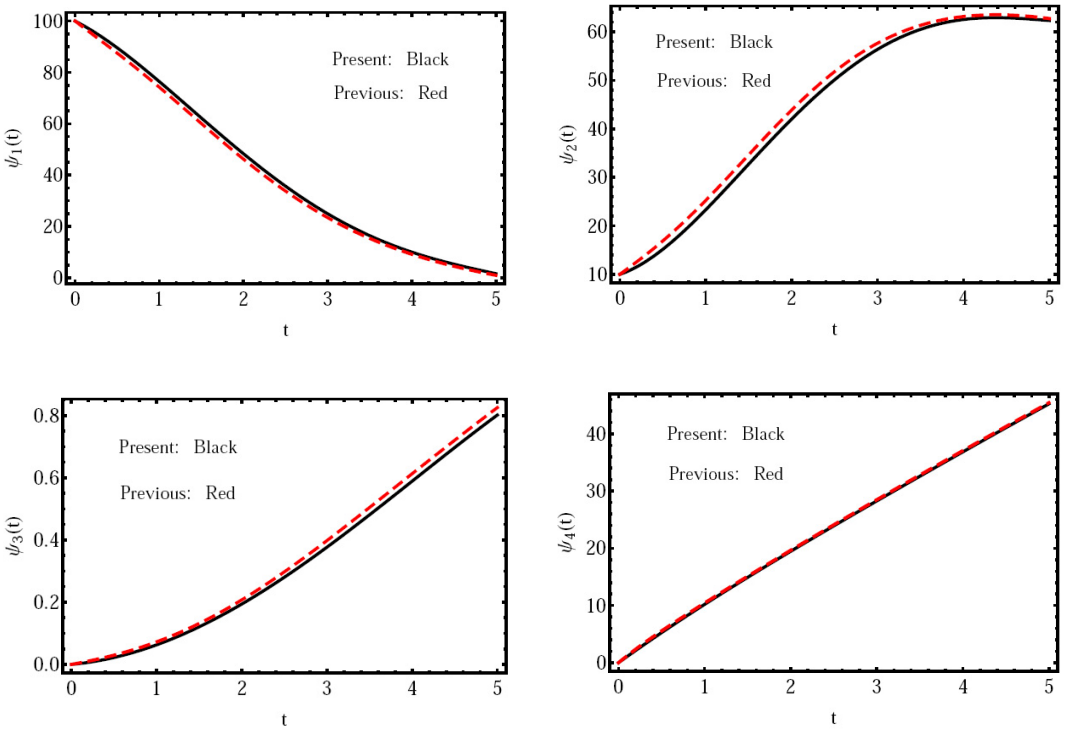

Figure 6. Comparison between the obtained numerical solution & the approximate solution [25] with the I.Cs given by Case 1.

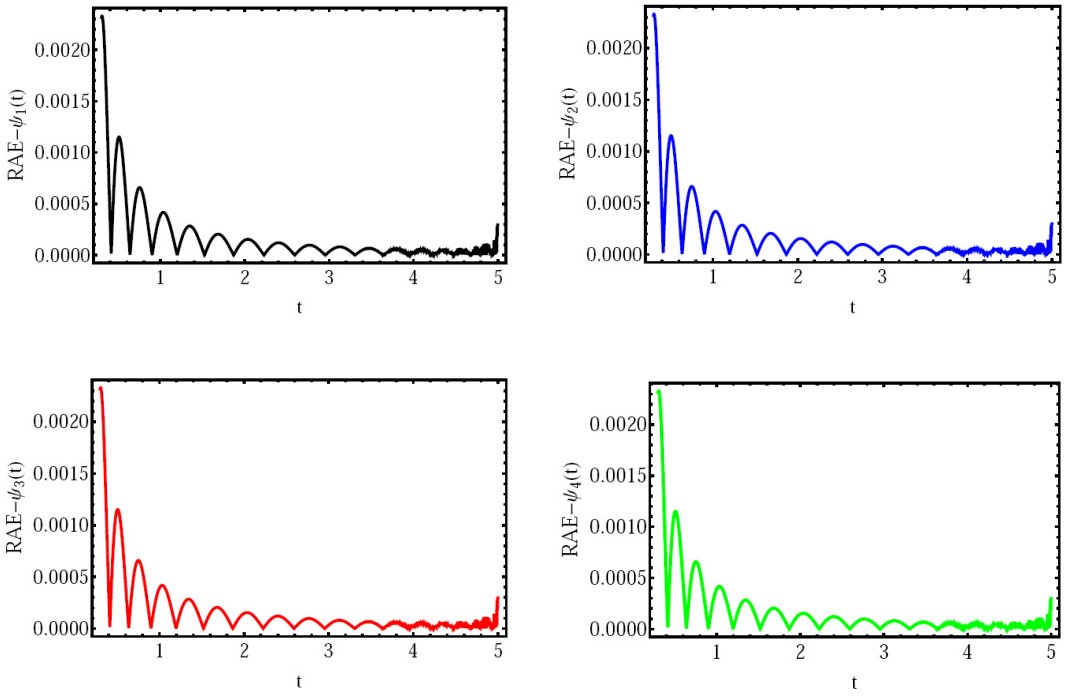

Figure 7. The RAE with $\nu = 0.95$ for the I.Cs given by Case 1.

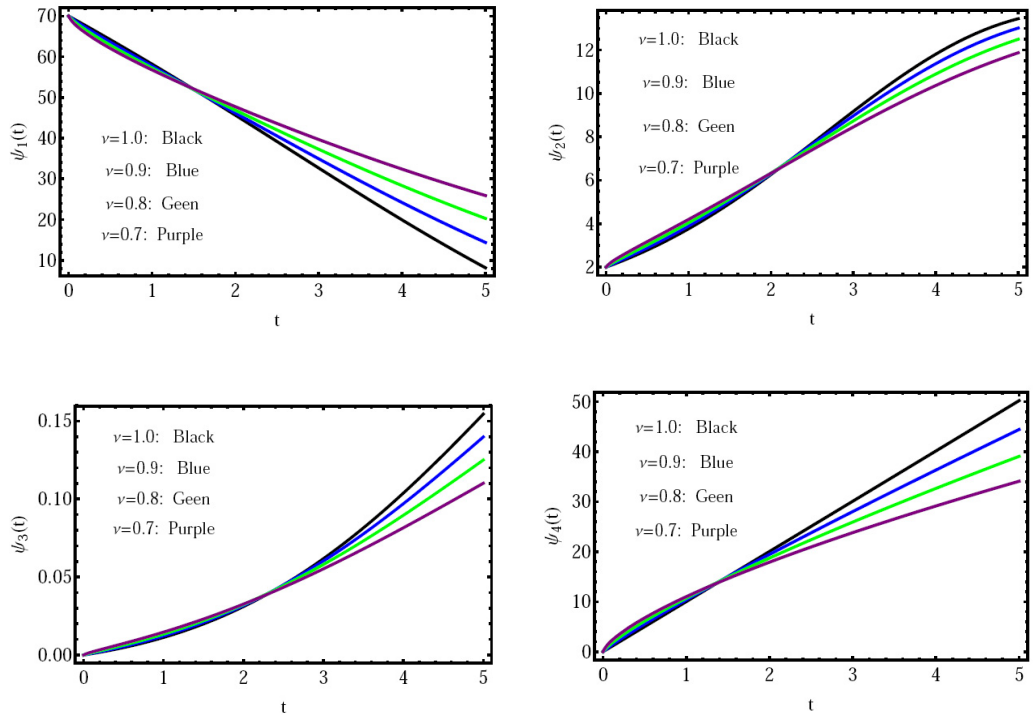

Figure 8. The influence of the fractional-order $\nu > 0.5$ on the numerical solution, using initial conditions given in Case 2.

By looking closely at these five figures, we can assert and confirm that the behavior of the numerical solution is based on the different amounts of ν, β, α, γ, δ, ϵ, n ; it is a clear indication that the presented numerical scheme has been well implemented to solve the given system in its fractional form with this type of derivatives with small and large values of the fractional order. In addition, we can also emphasize the efficiency of the suggested scheme and note that all studies related to convergence analysis have been achieved. Finally, the major and important observation is that the behavior of the numerical solutions agrees excellently with the real meaning of the problem and meets the same behavior of the system $\psi_k(t)$, $k = 1, 2, 3, 4$ through different values of these variables.

In addition, to verify the numerical convergence of the solutions in the interval $[0, 5]$, the FTR is applied to solve the given problem as the benchmarking to the proposed FSR in terms of efficiency and accuracy [10]. In Table 2, we computed the maximum AAE to show the performance of the FSR method against the benchmark method in solving the EVD model at various values of ν and h. Table 2 shows that the maximum AAE decreases when the step-size used in the computation decreases. Therefore, the errors illustrated sufficient proof of numerical convergence of the proposed numerical scheme. This comparison confirms the thoroughness of the proposed method in this article.

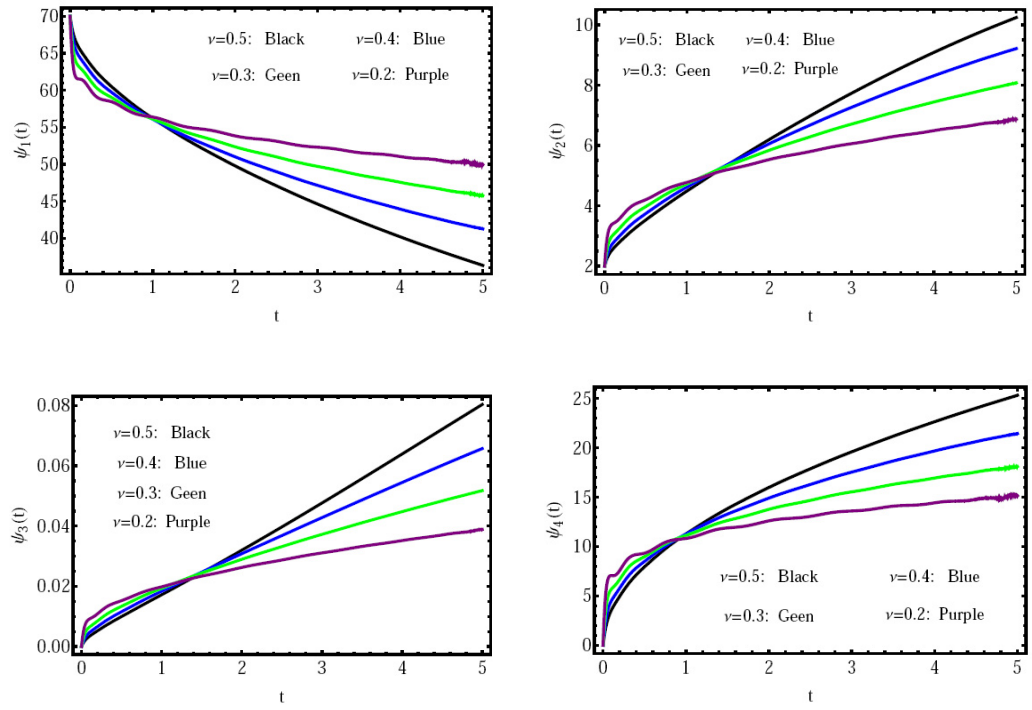

Figure 9. The influence of the fractional-order $\nu \leq 0.5$ on the numerical solution, using initial conditions given in Case 2.

Table 2. A comparison of the maximum absolute approximate errors from solving the EVD model at different values of ν, and h.

Method	ν/h	$\frac{1}{2}$	$\frac{1}{4}$	$\frac{1}{8}$	$\frac{1}{16}$	$\frac{1}{32}$
FSR	0.75	0.1345E-2	5.9510E-3	8.2140E-4	5.6064E-5	3.5641E-6
FTR		2.1593E-1	5.6542E-2	7.3571E-2	6.9510E-3	0.0145E-4
FSR	0.85	2.7562E-2	9.2458E-3	7.9630E-4	3.7532E-5	0.6528E-6
FTR		7.7530E-1	2.0147E-2	6.6529E-3	6.1597E-3	8.0581E-4
FSR	0.95	0.2580E-2	1.9507E-3	6.5219E-4	9.9425E-5	2.9324E-6
FTR		9.3520E-1	6.0147E-2	0.6541E-2	8.9327E-3	1.7538E-4

8. Conclusions and remarks

This study aims to utilize an efficient and accurate method to gain numerical solutions for CF-fractional blood ethanol concentration system and Ebola Virus model. Simpson's rule 1/3 was applied in its fractional form in computing the resulting integral within the system of FIEs corresponding to the FDEs expressing mathematically the models under study to achieve fourth-order accuracy for the resulting solutions. This study utilized several values of the fractional order and h to derive solutions for the models being examined. Furthermore, we have determined that the proposed approach is remarkably effective in

analyzing these systems. Furthermore, reducing the value of h allows us to control the accuracy of the numerical solution. From the obtained solutions, we can confirm that the offered approach is surprisingly successful in simulating the two models, as well as demonstrating the accuracy and computational effectiveness of this method. Finally, the present study may contribute to providing more robust physical explanations for future theoretical and computational studies on the same topic. In future work, we try to use other fractional operators and derive a suitable numerical scheme to solve a wide class of fractional differential equations such as complex, chaotic systems, or higher-dimensional systems.

References

[1] T. Abdeljawad and D. Baleanu. On fractional derivatives with exponential Kernel and their discrete versions. *Rep. Math. Phys.*, 80:11–27, 2017.

[2] J. F. G. Aguilar, H. Y. Martinez, C. C. Ramon, I. C. Ordunia, R. F. E. Jimenez, and V. H. O. Peregrino. Modeling of a mass-spring-damper system by fractional derivatives with and without a singular Kernel. *Entropy*, 17:6289–6303, 2015.

[3] N. Almutairi and S. Saber. Application of a time-fractal fractional derivative with a power-law kernel to the Burke-Shaw system based on Newton's interpolation polynomials. *MethodsX*, 12:1–13, 2024.

[4] S. B. Amundsen. Historical analysis of the Ebola virus: Prospective implications for primary care nursing today. *Clin. Excell. Nurse Pract.*, 2:343–351, 1998.

[5] I. Area, H. Batarfi, J. Losada, J. J. Nieto, W. Shammakh, and A. Torres. On a fractional order Ebola epidemic model. *Adv. Differ. Equ.*, 2015:1–8, 2015.

[6] S. Arshad, I. Saleem, A. Akgül, J. Huang, Y. Tang, and S. M. Eldin. A novel numerical method for solving the Caputo-Fabrizio fractional differential equation. *AIMS Mathematics*, 8:9535–9556, 2022.

[7] L. Baseler, D. S. Chertow, K. M. Johnson, H. Feldmann, and D. M. Morens. The pathogenesis of Ebola virus disease. *Ann. Rev. Pathol.*, 12:387–418, 2017.

[8] M. Caputo and M. Fabrizio. A new definition of fractional derivative without singular Kernel. *Progr. Fract. Differ. Appl.*, 1:73–85, 2015.

[9] M. A. Dokuyucu and H. Dutta. A fractional order model for the Ebola virus with the new Caputo fractional derivative without a singular Kernel. *Chaos Solitons Fract.*, 134:1–10, 2020.

[10] A. Jajarmi, S. Arshad, and D. Baleanu. A new fractional modeling and control strategy for the outbreak of dengue fever. *Physica A*, 535:1–10, 2019.

[11] M. M. Khader and M. Adel. Modeling and numerical simulation for covering the fractional COVID-19 model using spectral collocation-optimization algorithms. *Fractal and Fractional*, 6:1–19, 2022.

[12] M. M. Khader and K. M. Saad. Numerical treatment for studying the blood ethanol concentration systems with different forms of fractional derivatives. *Inter. J. Modern Physics C*, 31:1–10, 2020.

[13] M. M. Khader, N. H. Sweilam, A. M. S. Mahdy, and N. K. A. Moniem. Numerical simulation for the fractional SIRC model and influenza A. *Applied Mathematics and Information Sciences*, 8:1029–1036, 2014.

[14] J. Losada and J. J. Nieto. Properties of a new fractional derivative without singular Kernel. *Progr. Fract. Differ. Appl.*, 1:87–92, 2015.

[15] C. Ludwin. Blood alcohol content. *Undergrad. J. Math. Model.*, 3:1–10, 2011.

[16] G. K. Mazandu, V. Nembaware, N. E. Thomford, C. Bope, O. Ly, E. R. Chimusa, and A. Wonkam. A potential roadmap to overcome the current eastern DRC Ebola virus disease outbreak: From a computational perspective. *Sci. Afr.*, 7:1–10, 2020.

[17] P. A. Naik, M. Yavuz, S. Qureshi, M. Naik, K. M. Owolabi, A. Soomro, and A. H. Ganie. Memory impacts in hepatitis C: A global analysis of a fractional-order model with an effective treatment. *Computer Methods and Programs in Biomedicine*, 254:1–15, 2024.

[18] F. Ndairou, I. Area, J. J. Nieto, and D. F. M. Torres. Mathematical modeling of COVID-19 transmission dynamics with a case study of Wuhan. *Chaos Solitons Fract.*, 135:1–12, 2020.

[19] K. M. Owolabi and A. Atangana. Analysis and application of new fractional Adams-Bashforth scheme with Caputo-Fabrizio derivative. *Chaos Soliton. Fract.*, 105:111–119, 2017.

[20] S. Qureshi, I. K. Argyros, H. Jafari, A. Soomro, and K. Gdawiec. A highly accurate family of stable and convergent numerical solvers based on the Daftardar-Gejji and Jafari decomposition technique for systems of nonlinear equations. *MethodsX*, 13:1–24, 2024.

[21] S. Qureshi, A. Yusuf, A. A. Shaikh, M. Inc, and D. Baleanu. Fractional modeling of blood ethanol concentration system with real data application. *Chaos*, 29:1–16, 2019.

[22] A. Rachah and D. F. M. Torres. Mathematical modeling, simulation, and optimal control of the 2014 Ebola outbreak in West Africa. *Discr. Dyn. Nature Soc.*, 3:1–10, 2015.

[23] A. Rachah and D. F. M. Torres. Predicting and controlling the Ebola infection. *Math. Methods Appl. Sci.*, 40:6155–6164, 2017.

[24] S. Saber. Control of chaos in the Burke-Shaw system of fractal-fractional order in the sense of Caputo-Fabrizio. *J. Applied Mathematics and Computational Mechanics*, 23:83–96, 2024.

[25] H. M. Srivastava, K. M. Saad, and M. M. Khader. An efficient spectral collocation method for the dynamic simulation of the fractional epidemiological model of the Ebola virus. *Chaos, Solitons & Fractals*, 140:1–7, 2020.